

from that of the binary Al-Cu alloys and prevents formation of vacancy loops. It would also follow that the silicon atom vacancy association contributes to the zone formation during ageing, with a resultant GPB type zone of Al-Si-(Cu-Mg), rather than of a GPI (Al-Cu) zone.

GPB zones have also been noted [4] in the room temperature ageing of Al-2.5% Cu-1.2% Mg-0.24% Si, but in association with GPI zones. This result is consistent with the present findings as the partition of vacancies to silicon atoms was somewhat less favourable (~80%, cf.94%). The comparison may be further examined by utilizing the temperature dependence of the partition of vacancies given by Equation 2, as an increase in the ageing temperature of Al L70 to 130°C would reduce the partition of vacancies to silicon to 83%. Hence it is significant that GPI zones were tentatively identified during 130°C ageing of Al L70 and definitely established during higher temperature ageing (160 and 190°C).

These results suggest that the transformation from GPB zones to S' precipitate, which has not been hitherto observed in Al L70, may be favoured at ageing temperatures between room temperature and 130°C, with the consequent possibility of novel properties for this commercially significant alloy.

### Acknowledgements

The provision of an equipment and maintenance

grant (PKD) for this research by the Ministry of Defence (Procurement Executive) is gratefully acknowledged, together with the support of Mr C. R. Milne of the Avionics (now Radio and Navigation) Division, Royal Aircraft Establishment.

### References

1. W. BONFIELD and P. K. DATTA, *J. Mater. Sci.* **11** (1976) 1661.
2. P. K. DATTA, Ph.D. Thesis, University of London (1974).
3. J. M. SILCOCK, *J. Inst. Metals* **89** (1960) 203.
4. R. N. WILSON, *ibid* **97** (1969) 80.
5. K. H. WESTMACOTT, D. HULL, R. S. BARNES and R. E. SMALLMAN, *Phil. Mag.* **6** (1961) 929.
6. H. ROSENBAUM and D. TURNBULL, *Acta Met.* **7** (1959) 664.
7. G. THOMAS, *J. Inst. Metals* **90** (1961-62) 57.
8. D. W. PASHLEY, J. W. RHODES and A. SENDOREK, *ibid* **94** (1966) 41.
9. H. KIMURA and R. R. HASIGUTI, *Acta Met.* **9** (1961) 1076.

Received 3 November  
and accepted 22 November 1976

W. BONFIELD  
Department of Materials,  
Queen Mary College,  
London, UK

P. K. DATTA  
Department of Chemistry and Metallurgy,  
Glasgow College of Technology,  
Glasgow, UK.

### The topotactic decomposition of calcite group carbonates

The structural transformation which occurs in the decomposition of calcite group carbonates was reported [1] to exhibit conservation of the hexagonal layers, but elsewhere, [2], it was shown that the  $(10\bar{1}4)_c$  cleavage faces become the  $(110)_o$  plane family of the oxide. (c = carbonate, o = oxide). These two results are contradictory. In a study of the two-fold transformation of calcite crystals into oxide and then into hydroxide one of us [3] also found preferential orientations which cannot be explained by [1] and so a new study was appropriate.

The texture of the "pseudomorphs" which result from the decomposition of cadmium carbonate crystals has been completely investigated. The results of this investigation and their interpretation will be summarized here and these interpretations, supported by correlations between the two structures, will be published in more detail later [4].

The X-ray diffraction patterns of the decomposed crystals were obtained with the  $[001]_c$  axis of the habit oriented along the rotation axis of a cylindrical camera, and with no crystal oscillation occurring during the exposures. The layer-lines of the patterns (Fig. 1) reveal a fibre texture in which the fibre axis shows a "pseudo-triad symmetry".

Indeed, two patterns obtained after a 120° rotation of the pseudomorph around the  $[001]_c$  axis of the habit are identical but after a 60° rotation they are not. According to [1] it would be possible to postulate that the fibre axis is a triad axis of the oxide cubic lattice; however, the period deduced from the patterns agrees not with the  $a\sqrt{3}$  parameter according to a  $[111]_o$  axis, but with  $a\sqrt{17}$ .

To explain this “pseudo-symmetry” we suppose that it is a  $(h\bar{h}0l)_c$  family, non-rectangular with the triad axis, which is conserved during the transformation. There are two other equivalent families  $(oh\bar{h}l)_c$  and  $(\bar{h}ohl)_c$ . These three families are derived from one another by 120° rotations around  $[001]_c$ , and each of them can give rise to the  $(h'k'l')_o$  family. Thus the oxide crystallites can show three orientations at 120° from one another in the carbonate crystal habit while having the same  $[uvw]_o$  axis along  $[001]_c$ .

On the 200 diffraction ring (Fig. 1) there are two spots which are on the zero layer-line, so the fibre axis must be of the  $[uv0]$  type. The angles between the four 111 spots, which belong to two of the three oxide crystallite “populations”, and the angles they make with the fibre axis are seen in a stereographic projection of the CdO lattice directions (Fig. 2).  $[uv0]_o$  is in the equatorial plane

and at 45°30' and at 65°10' from two  $[111]$  type axes of the same “population”;  $[\bar{1}40]_o$  satisfies all of these conditions. The parameter of this direction agrees with the layer lines obtained in all the patterns.

According to the above supposition we have drawn the reciprocal  $(\bar{1}40)^*$  planes of three CdO lattices oriented at 120° from one another around  $[\bar{1}40]_o$ . Using the Ewald construction it was possible to index all the diffraction spots of the different patterns, and this agrees with the above hypothesis. For each pattern the orientation of the habit was well known, so the orientation of  $(\bar{1}40)_o$  of the three oxide “populations” about  $(00.1)_c$  of the habit was known precisely. The orientation relationships between the lattices of the three oxide “populations” designated A, B and C respectively, and the carbonate crystal lattice are given in Table I.

An SEM study of the oxide layer formed with respect to the natural faces of the carbonate crystal shows that the crystallites of the three orientations are not mixed in an aleatory manner; these three “populations” of oxide crystallites A, B and C are “disjointed” e.g. one domain of the crystal forms the population A, and the other two domains form B and C respectively.

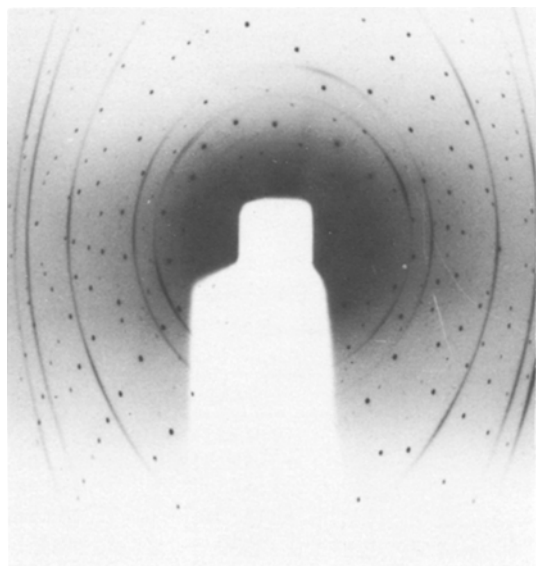


Figure 1 X-ray diffraction pattern of a CdCO<sub>3</sub> crystal after decomposition into CdO.

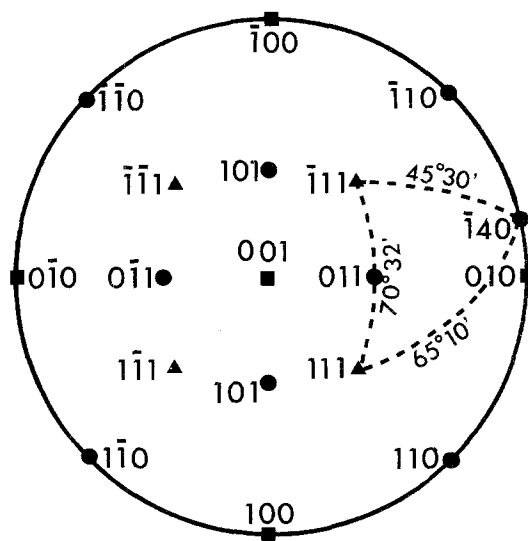


Figure 2 Stereographic projection of CdO axis - central pole  $[001]_o$ .

TABLE I Corresponding lattice planes in  $\text{CdCO}_3$ - $\text{CdO}$  transformation.  $\Delta\phi$  is the angle between the corresponding planes

$\text{CdCO}_3$ habit	Population A		Population B		Population C	
	( <i>hkl</i> )	$\Delta\phi$	( <i>hkl</i> )	$\Delta\phi$	( <i>hkl</i> )	$\Delta\phi$
(00.1)	( $\bar{1}40$ )	0	( $\bar{1}40$ )	0	( $\bar{1}40$ )	0
(01 $\bar{1}2$ )	( $\bar{1}00$ )	12°	(11 $\bar{1}$ )	20°	(111)	20°
( $\bar{1}012$ )	(111)	20°	( $\bar{1}00$ )	12°	(11 $\bar{1}$ )	20°
(1 $\bar{1}02$ )	(11 $\bar{1}$ )	20°	(111)	20°	( $\bar{1}00$ )	12°
( $\bar{1}104$ )	( $\bar{1}11$ )	2°	( $\bar{1}1\bar{1}$ )	2°	(110)	12°
(0 $\bar{1}14$ )	(110)	12°	( $\bar{1}11$ )	2°	( $\bar{1}1\bar{1}$ )	2°
(10 $\bar{1}4$ )	( $\bar{1}1\bar{1}$ )	2°	(110)	12°	( $\bar{1}11$ )	2°
(0 $\bar{1}11$ )	(210)	0				
(10 $\bar{1}1$ )			(210)	0		
( $\bar{1}101$ )					(210)	0
( $\bar{2}110$ )	(001)	0				
(1 $\bar{2}10$ )			(001)	0		
(11 $\bar{2}0$ )					(001)	0

### Acknowledgement

The authors are grateful for Drs R. Aumont, R. Lemaitre and P. Pouillen (Laboratoire pour

l'Étude des Propriétés Mécaniques et Thermodynamiques des Matériaux du C.N.R.S., Université de Paris XIII) who obligingly supplied the cadmium carbonate crystals.

### References

1. D. R. DASGUPTA, *Ind. J. Phys.* 38 (1964) 623.
2. R. SINGH DEV, *N. Jahrb. Min.* 1 (1972) 12.
3. J.-C. NIEPCE, Thesis, University of Dijon, France (1976).
4. N. FLOQUET and J.-C. NIEPCE, *ibid.*, to be published.

Received 17 November  
and accepted 16 December 1976

N. FLOQUET

J.-C. NIEPCE

Laboratoire de Recherche sur la Réactivité des Solides,  
Faculté des Sciences-Mirande,  
Campus Universitaire,  
Dijon, France

### Thermal expansion of indium borate

Under a programme of X-ray studies on calcite-type compounds, the authors have determined the precision lattice parameters and the coefficients of thermal expansion of a number of carbonates [1-4], nitrates [5] and borates [6]. A search of the literature shows that the thermal expansion of indium borate, which has the same structure as calcite, has not so far been studied. Hence it is thought worthwhile to include indium borate as part of a programme of X-ray studies on calcite-type compounds.

The sample used in the present study was supplied by the Mackway Company, New York. It was found necessary to heat the sample to 900°C to get well resolved sharp lines in the high angle region. The powder sample for the study was prepared by placing it in a thin-walled quartz capillary. The powder pattern showed few extra reflections, identified as being due to  $\text{In}_2\text{O}_3$ , as observed by Levin *et al.* [7]. Using a 19 cm high temperature camera, powder photographs were taken with Cu radiation at different temperatures ranging from 30 to 658°C. Five reflections

(2.2.12) $_{\alpha_1}$ , (3.1.14) $_{\alpha_1}$ , (3.1.14) $_{\alpha_2}$ , (4.1.10) $_{\alpha_1}$  and (4.1.10) $_{\alpha_2}$ , recorded in the Bragg angle region 61° and 79°, were used to evaluate the lattice parameters at different temperatures. The experimental details and the method of evaluating the precision lattice parameters and the coefficients of thermal expansion have been described in an earlier paper [1].

The lattice parameters determined at different temperatures are given in Table I. It can be seen that both the parameters *a* and *c* increase with temperature. The mean standard error of the lattice parameters, in the temperature range 30 to

Temperature (°C)	<i>a</i> (Å)	<i>c</i> (Å)
30	4.8224	15.4891
165	4.8261	15.5041
217	4.8289	15.5087
361	4.8336	15.5279
462	4.8378	15.5411
516	4.8399	15.5438
565	4.8407	15.5538
608	4.8422	15.5592
658	4.8441	15.5642